Networks and Heterogeneous Media

https://www.aimspress.com/journal/nhm

NHM, 21(3): 943–967.
DOI: 10.3934/nhm.2026039
Received: 26 January 2026
Revised: 19 February 2026
Accepted: 24 February 2026
Published: 12 May 2026

Research article

A Chelyshkov-based spectral homotopy analysis method for singular nonlinear Lane–Emden-type equations

Mouaad Bouakkaz[1,*], Nouria Arar[2], Mabrouk Meflah[1], Kamal Shah[3], Bahaaeldin Abdalla[3] and Thabet Abdeljawad[3,4,5,6,*]

[1] Laboratory of Applied Mathematics, Kasdi Merbah University, Ouargla 30000, Algeria

[2] Department of Mathematics, Constantine 1 University, Brothers Mentouri, Constantine 25017, Algeria

[3] Department of Mathematics and Sciences, Prince Sultan University, Riyadh 11586, Saudi Arabia

[4] Department of Fundamental Sciences, Faculty of Engineering and Architecture, Istanbul Gelisim University, Avcilar, Istanbul 34310, Turkey

[5] Department of Medical Research, China Medical University, Taichung 40402, Taiwan, China

[6] Department of Mathematics and Applied Mathematics, School of Science and Technology, Sefako Makgatho Health Sciences University, Ga-Rankuwa , South Africa

* **Correspondence:** Email: tabdeljawad@psu.edu.sa, bouakkaz.mouaad@univ-ouargla.dz.

Abstract: An enhanced numerical technique for solving the Lane–Emden equation is developed using the spectral homotopy analysis method (SHAM) with Chelyshkov polynomials and Gauss–Lobatto collocation nodes. The numerical results, including absolute errors and comparisons with the exact solution, demonstrate the convergence behavior and accuracy of the proposed approach. The results show that the Chelyshkov-based SHAM provides an effective framework for the numerical treatment of Lane–Emden-type problems.

Keywords: nonlinear equations; Lane–Emden equation; Chelyshkov polynomials; spectral methods; spectral homotopy analysis method

1. Introduction

The Lane–Emden equation plays a fundamental role in astrophysics, acting as a main mathematical base for the modeling of inner behaviors for self-gravitated objects and the spherical polytropic fluids. It gives a description about the balance between the gravity force, which pushes gas inward, and at the same time, the pressure that resists collapse. This kind of balance determines temperature, density, and

pressure spread in stars, and this shows that the Lane–Emden equation is important for studying the stability and evolution in stars [1–3].

Lane–Emden-type equations are generally expressed by [4]

$$y''(x) + \frac{\gamma}{x}y'(x) + \theta(x)\mu(y) = \varphi(x), \quad x > 0, \tag{1.1}$$

according to

$$y(0) = \lambda \quad \text{and} \quad y'(0) = \zeta,$$

where $\gamma \in \mathbb{R}_+, \lambda, \zeta \in \mathbb{R}$, and $\theta(x), \mu(y)$ and $\varphi(x)$ are predefined functions. Solving such nonlinear differential equations presents significant challenges due to their sensitivity to initial and boundary conditions and the absence of general analytical solutions for most cases [5–8]. Various numerical techniques have been applied to the Lane–Emden equation, including the Hermite functions collocation (HFC) method [4], extended Bernoulli wavelets (EBWs) [9], ultraspherical wavelets method [10, 11], modified Adomian method [12], two spectral Legendre's derivative [13], spectral Adomian decomposition (SADM) method [14], nonstandard finite difference (NSFD) technique [15], homotopy perturbation method with Laplace transform (LT-HPM) [16], Adomian decomposition method [17, 18], variational iteration method (VIM) [19], homotopy analysis method (HAM) [20], residual power series (RPS) method [21], and optimal homotopy asymptotic method [22], among other computational approaches. Additionally, spectral methods [23–26] have proven to be computationally efficient for nonlinear problems, often yielding superior accuracy and faster convergence across various applications [27–31]. Standard implementations of many semi-analytical and iterative numerical methods may encounter difficulties near $x = 0$ due to the presence of the singular coefficient x^{-1} [32]. In the proposed method, this issue is addressed through a spectral collocation treatment [33] in which the differential equation is enforced only at interior nodes, while the singular point is handled via regularity conditions.

By skipping over the singular point in total, this way gives essential numerical stabilization and more accurate results close by the origin. However, a real benefit that is visible is found in applying spectral methods. On the other hand, alternative non-spectral ways usually are blocked at algebraic convergence, but the use of spectral techniques causes exponential speed for smooth solutions, so it dramatically drops the computational work required. Among these methods, the spectral homotopy analysis method (SHAM) [34] combines the precise results using spectral techniques and flexibility from the HAM framework [35–38]. The main advancement shown here is by using Chelyshkov polynomials [39, 40] as foundation basis functions. Chelyshkov polynomials, unlike Legendre or Chebyshev bases, are by default orthogonal in the [0, 1] interval and satisfy the boundary condition at the origin smoothly. So, we can impose regularity at the singular point directly. In the practical sense, it means there is a strong improvement of numerical stability, and it is possible to get high-accuracy outcomes though the truncation order is much lower. In the long term, the SHAM based in Chelyshkov does not require linearization, assuming there are only small perturbations, but instead can handle the nonlinear Lane–Emden equation and remains reliable near singular points.

The rest of this article is organized as follows: Section 2 introduces Chelyshkov polynomials and brings out key properties for them, while Section 3 is about our computational system on the solution

we suggest. In Section 4, we present a rigorous analysis of errors with a comparison study among the exact and approximate solutions. The results show not only higher accuracy but also faster convergence compared to some existing methods. In addition, SHAM's inborn flexibility to handle parameters for controlling of convergence, makes it stronger and more adaptive as a tool to solve complicated problems of nonlinear nature in different domains in science and engineering. In the end, Section 5 closes the study by a summary of the main findings.

2. Key characteristics of Chelyshkov polynomials

Before going into main analysis, we briefly revisit fundamental properties of Chelyshkov polynomials. Chelyshkov first introduced these polynomials and established that they form a robust orthogonal system on the interval [0, 1]. For a given number N, basis functions are written clearly as follows:

$$C_{N,i}(t) = \sum_{s=0}^{N-i} (-1)^s \binom{N-i}{s} \binom{N+i+s+1}{N-i} t^{i+s}, \quad i = 0, 1, \ldots, N, \tag{2.1}$$

where $\binom{r}{s}$ is the standard notation of the binomial coefficient.

A notable property that makes this family computationally attractive is their easy generation via a recurrence relation. This allows the computational cost to remain similar to that of more common orthogonal sets, such as Chebyshev or Legendre polynomials. Moreover, their inherent orthogonality over [0, 1] provides a significant advantage when dealing with problems on semi-infinite domains, as they integrate seamlessly with standard domain transformation techniques. For the polynomial degrees considered in this study, no significant sensitivity to round-off errors has been observed.

The Chelyshkov polynomials meets the following orthogonality condition:

$$\int_0^1 C_{N,r}(t) C_{N,s}(t) \mathrm{dt} = \begin{cases} \frac{1}{r+s+1}, & \text{for } r = s, \\ 0, & \text{for } r \neq s, \end{cases} \qquad r, s = 0, 1, \cdots, N. \tag{2.2}$$

Chelyshkov polynomials $C_{Ni}(t)$ offer a natural approach for solving, expanding, and interpreting solutions. A function $y(t)$, square-integrable over the interval [0, 1], can be represented using Chelyshkov polynomials as

$$y(t_j) \approx y_N(t_j) = \sum_{i=0}^{N} e_i C_{N,i}(t_j), \quad j = 0, 1, \ldots, N. \tag{2.3}$$

Also,

$$\begin{aligned} y'_N(t_j) &= \sum_{i=0}^{N} e_i C'_{N,i}(t_j), \\ y''_N(t_j) &= \sum_{i=0}^{N} e_i C''_{N,i}(t_j), \quad j = 0, 1, \ldots, N, \end{aligned} \tag{2.4}$$

where e_i are the unknown coefficients, $C_{N,i}$, $i = 0, 1, \ldots, N$ represent the Chelyshkov orthogonal polynomials of degree N (with $N = 2, 3, \ldots$), and $t_0, t_1, \ldots, t_N$ are the Gauss–Lobatto collocation points, expressed as

$$t_j = \frac{1 + \cos\left(\frac{\pi j}{N}\right)}{2}, \quad j = 0, 1, \ldots, N. \tag{2.5}$$

3. Background of Chelyshkov-based SHAM

In the application of SHAM [34, 41–44], we focus on the nonlinear differential equation

$$\mathcal{L}(y(x)) + \mathcal{N}(y(x)) = f(x), \qquad a \le x \le b, \tag{3.1}$$

where $\mathcal{L}$ and $\mathcal{N}$ are the linear and nonlinear operators, respectively, and $f(x)$ is a known function.

The initial solution, denoted as $y_0(x)$, is chosen such that it satisfies Eq (3.2). This selection ensures that $y_0(x)$ provides a good approximation to the exact solution

$$\mathcal{L}\left(y_0(x)\right) = f(x) \tag{3.2}$$

and verifies the condition

$$B\left(y_0(x), y_0'(x), \ldots\right) = 0, \quad a \le x \le b, \tag{3.3}$$

where B is a linear operator. Within the context of HAM [35, 38], the equation representing the deformation at order 0 is expressed as

$$(1-\varrho)\mathcal{L}\left(\mathcal{Y}(x;\varrho) - y_0(x)\right) = \varrho c_0 \left(\mathcal{L}(\mathcal{Y}(x;\varrho)) + \mathcal{N}(\mathcal{Y}(x;\varrho)) - f(x)\right), \varrho \in [0,1], \tag{3.4}$$

where $0 \le \varrho \le 1$ is a parameter of embedding, c_0 is the convergence-control parameter and $\mathcal{Y}(x;\varrho)$ is an unknown function that deforms $y_0(x)$ into $y(x)$ as ϱ varies from 0 to 1.

Expanding $\mathcal{Y}(x;\varrho)$ in a Taylor series with respect to $\varrho \in [0,1]$, we obtain

$$\mathcal{Y}(x;\varrho) = y_0(x) + \sum_{k=1}^{\infty} y_k(x)\,\varrho^k, \tag{3.5}$$

where

$$y_k(x) = \frac{1}{k!}\left.\frac{\partial^k \mathcal{Y}(x,\varrho)}{\partial \varrho^k}\right|_{\varrho=0}. \tag{3.6}$$

Assuming that $\mathcal{L}$, $y_0(x)$, and c_0 are properly chosen such that the series converges at $\varrho = 1$, the homotopy-series solution is

$$\mathcal{Y}(x;1) = y_0(x) + \sum_{k=1}^{+\infty} y_k(x), \tag{3.7}$$

which satisfies the original Eq (3.1).

The deformation equation of order k is given by

$$\mathcal{L}\left(y_k(x) - (\delta_k + c_0)\, y_{k-1}(x)\right) = c_0 R_{k-1}\left(x\right), \tag{3.8}$$

where

$$R_{k-1}\left(x\right) = \frac{1}{(k-1)!}\left.\frac{\partial^{k-1}\left(\mathcal{N}(\mathcal{Y}(x;\varrho)) - f(x)\right)}{\partial \varrho^{k-1}}\right|_{\varrho=0} \tag{3.9}$$

and

$$\delta_k = \begin{cases} 0, & k \le 1, \\ 1, & k \ge 2. \end{cases} \tag{3.10}$$

The spectral method is carried out on the interval $[a, b]$ by introducing the transformation $x = (b-a)t + a$, valid for $a \le x \le b$. This allows us to rewrite the solution given in Eq (2.3) and its derivative Eq (2.4) in matrix form at the collocation points:

$$\begin{aligned}
\boldsymbol{\mathcal{Y}} &= \boldsymbol{C}(t)\boldsymbol{E}; \quad C(t) = \left(C_{Ni}(t_j)\right)_{0\le i,j\le N}, \\
\boldsymbol{\mathcal{Y}}' &= \frac{1}{b-a}\frac{d\boldsymbol{C}(t)}{dt}\boldsymbol{E}; \quad \frac{dC(t)}{dt} = \left(\frac{dC_{Ni}(t)}{dt}\right)_{0\le i\le N}, \\
\boldsymbol{\mathcal{Y}}'' &= \frac{1}{(b-a)^2}\frac{d^2\boldsymbol{C}(t)}{dt^2}\boldsymbol{E}; \quad \frac{dC(t)}{dt} = \left(\frac{d^2C_{Ni}(t)}{dt^2}\right)_{0\le i\le N},
\end{aligned} \tag{3.11}$$

where

$$\boldsymbol{\mathcal{Y}} = [y(x_0), \cdots, y(x_N)]^T, \ \boldsymbol{E} = [a_0, \cdots, a_N]^T, \text{ and } \boldsymbol{C}(t) = [C_{N0}(t)\ C_{N1}(t) \cdots C_{NN}(t)].$$

Substituting Eqs (2.3) and (3.11) in Eq (3.8), we obtain

$$\mathcal{B}E_k = (\delta_k + c_0)\mathcal{B}E_{k-1} + c_0\mathcal{R}, \tag{3.12}$$

where $\mathcal{B}$ and $\mathcal{R}$ denote the matrix and vector, respectively, resulting from the application of the Chelyshkov transformations Eqs (2.3) and (3.11) to $\mathcal{L}$ and R_{k-1}, respectively. Moreover,

$$\mathbf{E}_k \ = \ (e_{k_0}, e_{k_1}, \ldots, e_{k_N})^T. \tag{3.13}$$

By appropriately imposing the boundary conditions in Eq (3.12), we obtain

$$\mathcal{B}E_k = (\delta_k + c_0)\bar{\mathcal{B}}E_{k-1} + c_0\bar{\mathcal{R}}, \tag{3.14}$$

where $\bar{\mathcal{B}}$ and $\bar{\mathcal{R}}$ represent the modified matrix and vector, respectively, resulting from the implementation of the conditions at the boundaries on the right-hand side of Eq (3.12).

Therefore,

$$E_k = (\delta_k + c_0)\mathcal{B}^{-1}\bar{\mathcal{B}}E_{k-1} + c_0\mathcal{B}^{-1}\bar{\mathcal{R}}. \tag{3.15}$$

Here, $\mathcal{B}^{-1}$ denotes the inverse of the matrix $\mathcal{B}$. Equation (3.15) defines an iterative relation that facilitates the computation of k-th order approximation $E_k, k \ge 1$.

The following transformation is introduced to guarantee homogeneous boundary conditions [41–44]:

$$y(x) = u(t) + y_0(x). \tag{3.16}$$

Substituting Eq (3.16) into Eq (3.1) yields

$$\mathcal{L}(u(t)) + \mathcal{N}(u(t)) = \mathscr{H}(x),$$

subject to

$$P\left(u(t), u'(t), \ldots\right) = 0, \quad t = \frac{x-a}{b-a}, \quad a \le x \le b,$$

where P is a linear operator, and

$$\mathscr{H}(x) = f(x) - \mathcal{L}(y_0(x)) - \mathcal{N}(y_0(x)).$$

Then, the zero-th order deformation equation within the context of HAM becomes

$$(1-\varrho)\mathcal{L}(\mathcal{U}(t;\varrho) - u_0(t)) = \varrho c_0 (\mathcal{L}(\mathcal{U}(t;\varrho)) + \mathcal{N}(\mathcal{U}(t;\varrho)) - \mathscr{H}(x)), \quad 0 \le \varrho \le 1,$$

where $\mathcal{U}(x;\varrho)$ is an unknown function. The deformation equation of order k reads

$$\mathcal{L}(u_k(t) - (\delta_k + c_0)\, u_{k-1}(t)) = c_0 R_{k-1}, \tag{3.17}$$

where

$$R_{k-1} = \frac{1}{(k-1)!} \frac{\partial^{k-1} (\mathcal{N}(\mathcal{U}(t;\varrho)) - \mathscr{H}(x))}{\partial \varrho^{k-1}}\bigg|_{\varrho=0}.$$

Hence, the homotopy series solution is

$$y(x) = y_0(x) + u_0(t) + \sum_{k=1}^{+\infty} u_k(t). \tag{3.18}$$

The starting approximation $u_0(x)$ is obtained by solving the equation

$$\mathcal{L}(u_0(t)) = \mathscr{H}(x), \tag{3.19}$$

with

$$u_0(0) = u_0'(0) = 0. \tag{3.20}$$

To solve Eq (3.19), we use the Chelyshkov spectral collocation method, so

$$\mathbf{B}A_0 = \mathbf{H}, \tag{3.21}$$

subject to

$$\mathbf{U}_0(0) = \mathbf{U}_0'(0) = 0, \tag{3.22}$$

where

$$\begin{aligned} \mathbf{U}_0 &= \mathbf{C}(t)A_0, \\ \mathbf{H} &= (\mathscr{H}(x_0), \mathscr{H}(x_1), \ldots, \mathscr{H}(x_N))^T. \end{aligned}$$

By following the same procedure that led to Eq (3.15), we derive

$$\begin{cases} \boldsymbol{A}_0 = \mathcal{B}^{-1}\bar{\mathbf{H}}, \\ \boldsymbol{A}_k = (\delta_k + c_0)\mathcal{B}^{-1}\bar{\mathcal{B}}\boldsymbol{A}_{k-1} + c_0\mathcal{B}^{-1}\bar{\mathcal{R}}. \end{cases} \tag{3.23}$$

Equation (3.23) thus defines an iterative relation that facilitates the computation of k-th order approximations $A_k, k \ge 1$.

$$\begin{aligned} \boldsymbol{U} &= \boldsymbol{C}(t)\boldsymbol{A}, \\ \mathbf{A}_k &= (a_{k_0}, a_{k_1}, \ldots, a_{k_N})^T, \\ \boldsymbol{U} &= (u(t_0), u(t_1), \ldots, u(t_N))^T. \end{aligned} \tag{3.24}$$

4. Numerical tests

We now consider the use of Chelyshkov-based SHAM for solving Lane–Emden-type equations. The performance of the method is assessed by calculating the absolute error through the expression:

$$\mathcal{E} = \max_j \left| y(x_j) - y_M(x_j) \right|, \quad j = 0, 1, \ldots, N. \tag{4.1}$$

To analyze the numerical convergence behavior, the convergence rate is estimated based on the error as follows:

$$O = \frac{\log(\mathcal{E}(M_1)) - \log(\mathcal{E}(M_2))}{\log(M_1) - \log(M_2)}, \tag{4.2}$$

where $\mathcal{E}(M)$ represents the error calculated for two orders $M_1 \neq M_2$. In our tests, we have chosen $M_2 = M_1 + 1$, with $M_1 \geq 1$.

Computational performance and memory usage

All numerical experiments were conducted in MATLAB R2015a (Version 8.5) on a 64-bit Microsoft Windows 10 Professional Education system. The computations were carried out on a personal computer equipped with an Intel(R) Celeron(R) CPU 1005M @ 1.90 GHz (2 cores, 2 logical processors) and 8 GB of RAM.

During the simulations, MATLAB utilized approximately 1.75 GB of memory, while the maximum allowable array size was about 3.68 GB, indicating that the computations remained well within the available hardware limits. By using compacted spectral outcomes based on Chelyshkov polynomials, the Chelyshkov-based SHAM works with much less memory compared with other grid-based techniques like finite difference method. Even as the number of collocation points N increases, the computational burden remains in manageable ranges for simulations about astrophysics on large scales. For practical use, these Chelyshkov polynomials were generated using their recursive formulas in MATLAB codes. Matrix inversions and similar operations were done by the native "inv" command, which shows that the full algorithm is able to run efficiently and without requiring any additional toolboxes.

4.1. Nonlinear case

Problem 1

We focus on a Lane–Emden-type model described by:

$$y'' + \frac{2}{x}y' + y^2 = e^{x^2}(6 + 4x^2) + e^{2x^2}, \quad x \in (0, L]. \tag{4.3}$$

This problem is equipped with the values $y(0) = 1$ and $y'(0) = 0$ at the origin. Its exact solution is given by $y(x) = \exp(x^2)$. The linear and nonlinear operators are considered as follows:

$$L(y) = y'' + \frac{2}{x}y', \qquad N(y) = y'' + \frac{2}{x}y' + y^2.$$

To simplify the numerical treatment, we rescale the domain $[0, L]$ to the unit interval $[0, 1]$ via the transformation

$$x = Lt, \quad t \in [0, 1]. \tag{4.4}$$

Applying the following substitution:

$$y(x) = y_0(x) + u(t), \tag{4.5}$$

with $y_0(x) = x^2 + 1$ taken as an initial approximation, and inserting it into Eq (4.3), we arrive at

$$\frac{1}{L^2}u'' + \frac{2}{Lx}u' + 2y_0u + u^2 = \mathscr{H}(x), \tag{4.6}$$

accompanied by the conditions:

$$u(0) = u'(0) = 0,$$

and the source term $\mathscr{H}(x)$ is defined as:

$$\mathscr{H}(x) = -y_0'' - \frac{2}{x}y_0' - y_0^2 + e^{x^2}(6 + 4x^2) + e^{2x^2}.$$

Accordingly, the modified linear and nonlinear operators are given by

$$\mathcal{L}(u) = \frac{1}{L^2}u'' + \frac{2}{Lx}u' + 2y_0u, \qquad \mathcal{N}(u) = \frac{1}{L^2}u'' + \frac{2}{Lx}u' + 2y_0u + u^2.$$

By replacing $\mathscr{H}$, $\mathcal{L}$, and $\mathcal{N}$ in Eq (3.17), we have

$$\mathcal{L}(u_k) = (\delta_k + c_0)\mathcal{L}(u_{k-1}) + c_0\left[-(1 - \delta_k)\mathscr{H} + \sum_{i=0}^{k-1} u_i u_{k-i-1}\right] \tag{4.7}$$

such that $\mathcal{L}(u_0)$ is given by Eq (3.19) and

$$u_k(0) = u_k'(0) = 0. \tag{4.8}$$

Using Eqs (2.3) and (3.11), Eq (4.7) becomes

$$\mathbf{B}\mathbf{A}_k = (\delta_k + c_0)\mathbf{B}\mathbf{A}_{k-1} + c_0\left[-(1 - \delta_k)\mathbf{H} + \sum_{i=0}^{k-1}(\mathbf{C}(t)\mathbf{A}_i) \circ (\mathbf{C}(t)\mathbf{A}_{k-i-1})\right], \tag{4.9}$$

where $\circ$ denotes the element-wise product and

$$\mathbf{B} = \frac{1}{L^2}\mathbf{C}''(t) + \mathbf{diag}\left(\frac{2}{Lx}\right)\mathbf{C}'(t) + 2\mathbf{diag}(y_0),$$
$$\mathbf{A}_k = (a_{k_0}, a_{k_1}, ..., a_{k_N})^T.$$

Imposing initial conditions (4.8) appropriately in Eq (4.9) yields

$$\begin{cases} \mathbf{A}_0 = \mathbf{B}^{-1}\bar{\mathbf{H}}, \\ \mathbf{A}_k = (\delta_k + c_0)\mathbf{B}^{-1}\bar{\mathbf{B}}\mathbf{A}_{k-1} + c_0\mathbf{B}^{-1}\left[-(1 - \delta_k)\bar{\mathbf{H}} + \sum_{i=0}^{k-1}(\mathbf{C}(t)\mathbf{A}_i) \circ (\mathbf{C}(t)\mathbf{A}_{k-i-1})\right], \end{cases} \tag{4.10}$$

where

$$\left(\bar{\mathbf{B}}\right)_{i,j} = \begin{cases} (\mathbf{B})_{i,j}, & 2 \le i \le N, \\ 0, & i = 0, 1, \end{cases} \quad 0 \le j \le N; \text{ and } \bar{\mathbf{H}}_{\mathbf{j}} = \begin{cases} \mathbf{H}_j, & 2 \le j \le N, \\ 0, & j = 0, 1. \end{cases}$$

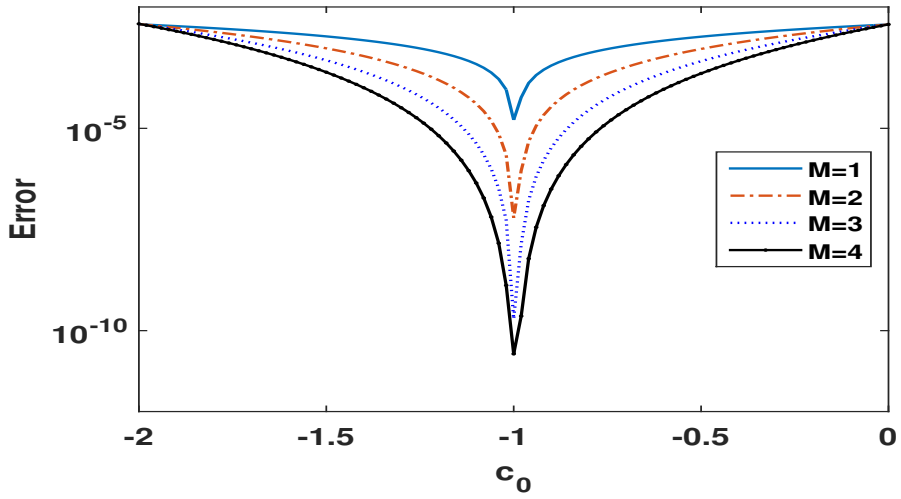

Figure 1. Error as a function of c_0 for Eq (4.3).

Figure 1 presents error curves that aid in determining the optimal value of the parameter that controls convergence c_0 with $N = 15$ and $L = 1$.

Table 1. Evaluating the Chelyshkov-based SHAM against the exact solution for the case $L = 1$, $c_0 = -1$, and $N = 15$ for Eq (4.3).

x	$M = 1$	$M = 2$	$M = 4$	Exact sol
0	1.00000000000000	1.00000000000000	1.00000000000000	1.00000000000000
0,01	1.00011938907242	1.00011938894818	1.00011938896677	1.00011938896472
0,04	1.00187034453095	1.00187034379048	1.00187034390147	1.00187034388881
0,1	1.00916032921094	1.00916032832890	1.00916032846104	1.00916032844618
0,17	1.02774660113385	1.02774660020471	1.02774660034397	1.02774660032811
0,5	1.06449445973407	1.06449445879269	1.06449445893373	1.06449445891786
0,35	1.12678041888148	1.12678041794720	1.12678041808730	1.12678041807137
0,45	1.22197367614868	1.22197367525722	1.22197367539461	1.22197367537915
0,55	1.35661928015897	1.35661928003518	1.35661928016785	1.35661928015284
0,65	1.53477127780161	1.53477128942213	1.53477128954642	1.53477128953225
0,75	1.75505453728019	1.75505465692595	1.75505465697248	1.75505465696030
0,83	2.00671465091321	2.00671537910942	2.00671537833900	2.00671537832539
0,9	2.26626784181401	2.26627071568976	2.26627071000402	2.26627070998778
0,96	2.49780172524407	2.49780928894393	2.49780926730229	2.49780926727809
0,99	2.65982927948423	2.65984273935667	2.65984269168939	2.65984269166280
1	2.71826558975603	2.71828189041310	2.71828182847822	2.71828182845905

Table 1 displays numerical results produced by applying the Chelyshkov-based SHAM across different approximation levels, alongside the corresponding exact values. This comparison demonstrates high accuracy of the method while using minimal computational resources, so its reliability for solving such equations is increased.

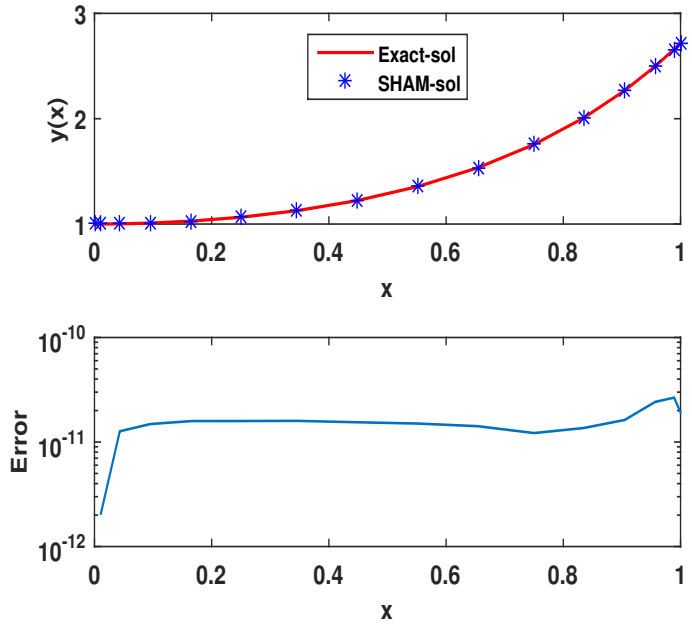

Figure 2. Exact vs. approximate solution with absolute error for $M = 4, N = 15, L = 1$, and $c_0 = -1$ for Eq (4.3).

Figure 2 shows a comparison among calculated and analytical solutions. It is observed that the two curves almost entirely coincide, which means that the method gives out extraordinary precision. It is supported in the next plot of absolute error, where the graph keeps nearly flat, and stays very close at zero in the region, pointing out the correctness and efficiency for the used method.

Table 2. Error norm and the order of convergence when $N = 15$ and $L = 1$ for Eq (4.3).

Order (M)	c_0	$\mathcal{E}$	O
1	-1	1.62387×10^{-05}	-8.03402
2	-1	6.19541×10^{-08}	-14.20895
3	-1	1.94984×10^{-10}	-6.92565
4	-1	2.65898×10^{-11}	———

Table 2 illustrates the error and convergence rate as the parameter c_0 varies with the order M, varying from 1 to 4. The results indicate good convergence, confirming the efficiency and reliability of the Chelyshkov-based SHAM.

Figure 3 confirms the spectral behavior of the Chelyshkov-based SHAM. Figure 3a shows the absolute error $\mathcal{E}$ as a function of the order M. The error decreases rapidly with increasing M, illustrating the exponential convergence of the Chelyshkov-based SHAM approach using Chelyshkov polynomials.

Even at moderate orders, the error reaches values on the order of 10^{-11}, confirming the high accuracy of the method. Figure 3b depicts the order of convergence $|O|$ versus M. The high values of $|O|$ for the initial orders indicate a rapid increase in accuracy as M increases, highlighting the spectral properties and stability of the Chelyshkov-based SHAM.

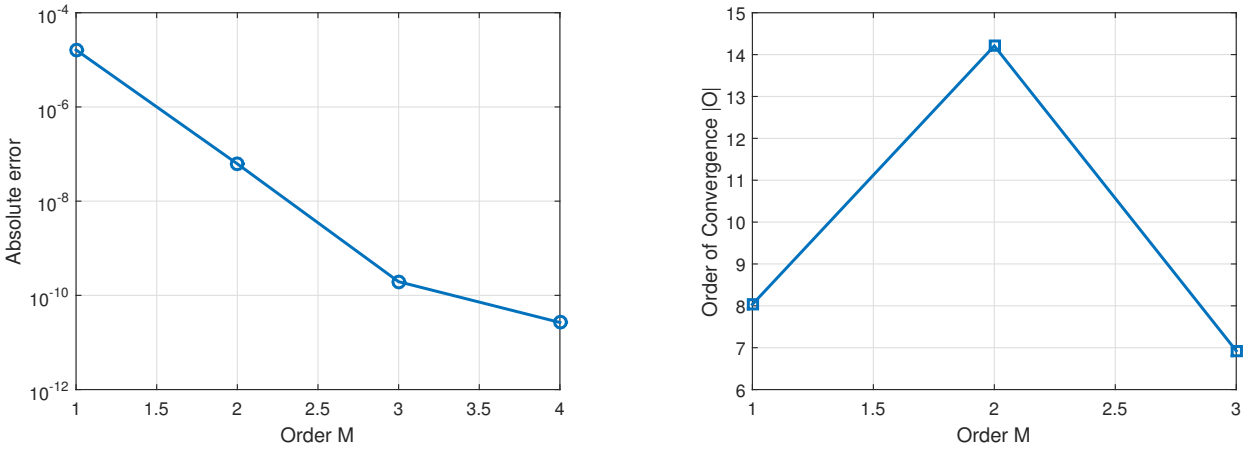

(a) Absolute error vs truncation order M.

(b) Order of convergence O vs M.

Figure 3. Spectral convergence behavior of Eq (4.3).

Problem 2

Consider the nonlinear differential equation defined in [16]:

$$y'' + \frac{2}{x}y' + y^3 = 6 + x^6, \quad x \in (0, L], \tag{4.11}$$

where $y(0) = 0,\ y'(0) = 0$ and $y(x) = x^2$. Using the relation (4.5) gives:

$$\frac{1}{L^2}u'' + \frac{2}{Lx}u' + 3y_0^2u + 3y_0u^2 + u^3 = g(x), \tag{4.12}$$

with

$$u(0) = u'(0) = 0,$$

where

$$\mathscr{H}(x) = -y_0'' - \frac{2}{x}y_0' - y_0^3 + 6 + x^6,$$

and $y_0(x) = x^2 + \frac{x^8}{72}$ is chosen as a solution of the linear part of Eq (4.11). The modified linear operator and the corresponding nonlinear operator are defined as:

$$\mathcal{L}(u) = \frac{1}{L^2}u'' + \frac{2}{Lx}u' + 3y_0^2u, \qquad \mathcal{N}(u) = \frac{1}{L^2}u'' + \frac{2}{Lx}u' + 3y_0^2u + 3y_0u^2 + u^3.$$

By replacing $\mathscr{H}$, $\mathcal{L}$, and $\mathcal{N}$ in Eq (3.17) , we have

$$\mathcal{L}(u_k) = (\delta_k + c_0)\mathcal{L}(u_{k-1}) + c_0\left[-(1-\delta_k)\mathscr{H} + 3y_0^2\sum_{i=0}^{k-1}u_iu_{k-i-1} + \sum_{i=0}^{k-1}\sum_{p=0}^{i}u_pu_{i-p}u_{k-i-1}\right]. \tag{4.13}$$

Using Eqs (2.3) and (3.11), the Eq (4.13) becomes:

$$\begin{aligned}\mathbf{BA}_k &= (\delta_k + c_0)\mathbf{BA}_{k-1} + c_0\Bigg[-(1-\delta_k)\mathbf{H} + 3y_0\sum_{i=0}^{k-1}(\mathbf{C}(t)\mathbf{A}_i)\circ(\mathbf{C}(t)\mathbf{A}_{k-i-1}) \\ &\quad + \sum_{i=0}^{k-1}(\mathbf{C}(t)\mathbf{A}_{k-i-1})\sum_{p=0}^{i}(\mathbf{C}(t)\mathbf{A}_{i-p})\circ(\mathbf{C}(t)\mathbf{A}_p)\Bigg],\end{aligned}$$

where

$$\mathbf{B} = \frac{1}{L^2}\mathbf{C}''(t) + \mathbf{diag}(\frac{2}{Lx})\mathbf{C}'(t) + 3\mathbf{diag}(y_0^2).$$

In the end, we find this system:

$$\begin{cases}\mathbf{A}_0 = \mathbf{B}^{-1}\bar{\mathbf{H}}, \\ \mathbf{A}_k = (\delta_k + c_0)\mathbf{B}^{-1}\bar{\mathbf{B}}\mathbf{A}_{k-1} + c_0\mathbf{B}^{-1}\Bigg[-(1-\delta_k)\bar{\mathbf{H}} + 3y_0\sum_{i=0}^{k-1}(\mathbf{C}(t)\mathbf{A}_i)\circ(\mathbf{C}(t)\mathbf{A}_{k-i-1}) \\ \qquad + \sum_{i=0}^{k-1}(\mathbf{C}(t)\mathbf{A}_{k-i-1})\sum_{p=0}^{i}(\mathbf{C}(t)\mathbf{A}_{i-p})\circ(\mathbf{C}(t)\mathbf{A}_p)\Bigg].\end{cases} \tag{4.14}$$

Table 3. Error $\mathcal{E}$ and the order of convergence when $N = 8$ and $L = 1$ for Eq (4.11).

Order (M)	c_0	$\mathcal{E}$	O
1	-1	3.15242×10^{-09}	-9.77852
2	-1	3.58935×10^{-12}	-16.77144
3	-1	3.99680×10^{-15}	-14.09029
4	-1	6.93889×10^{-17}	———

Table 3 displays rate of convergence O, and error value $\mathcal{E}$, with its associated optimal parameter c_0 when order M grows from 1 to 4. Reported outcomes show consistent converging, highlighting the accuracy and robustness of the Chelyshkov-based SHAM.

Table 4. Error variation for $M = 1, 2, 3$, and 4 with $c_0 = -1$, $L = 1$, and $N = 8$ for Eq (4.11).

x	$M = 1$	$M = 2$	$M = 3$	$M = 4$
0.038	2.17409×10^{-10}	1.88135×10^{-13}	2.04481×10^{-16}	1.04083×10^{-17}
0.146	1.28739×10^{-09}	1.11298×10^{-12}	1.21084×10^{-15}	6.24501×10^{-17}
0.309	1.54188×10^{-09}	1.34134×10^{-12}	1.45717×10^{-15}	6.93889×10^{-17}
0.5	1.62489×10^{-09}	1.46744×10^{-12}	1.55431×10^{-15}	5.55111×10^{-17}
0.691	1.67594×10^{-09}	1.69353×10^{-12}	1.83187×10^{-15}	5.55112×10^{-17}
0.854	1.85855×10^{-09}	2.14395×10^{-12}	2.33147×10^{-15}	0
0.962	2.56109×10^{-09}	2.98483×10^{-12}	3.33067×10^{-15}	0
1	3.15242×10^{-09}	3.58935×10^{-12}	3.99680×10^{-15}	0

Table 4 shows the variation of order M from 1 to 4. The results clearly show that there is a very significant error decreasing as the order increases, indicating that the Chelyshkov-based SHAM effectively improves accuracy over the interval [0, 1].

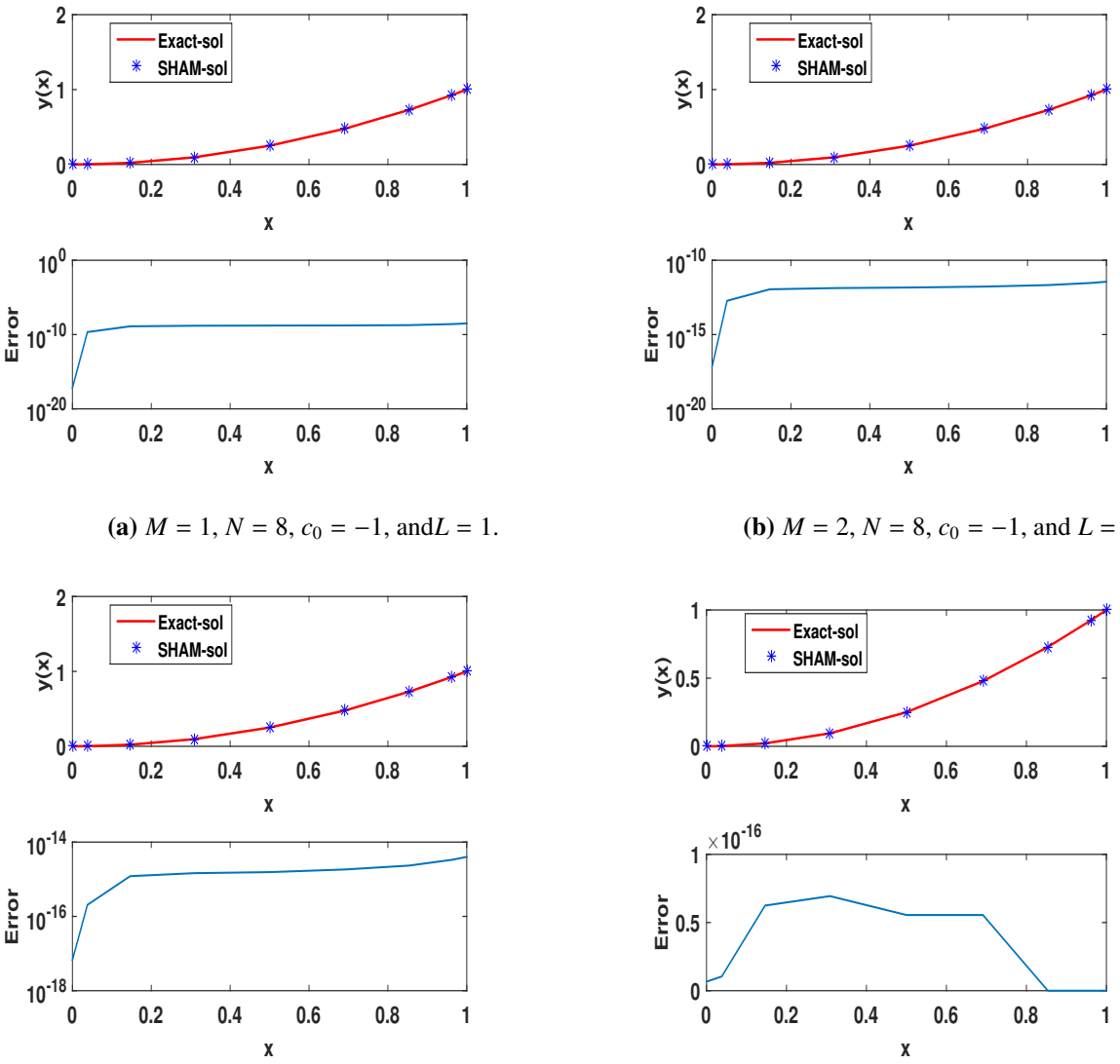

(a) $M = 1$, $N = 8$, $c_0 = -1$, and$L = 1$.

(b) $M = 2$, $N = 8$, $c_0 = -1$, and $L = 1$.

(c) $M = 3$, $N = 8$, $c_0 = -1$, and $L = 1$.

(d) $M = 4$, $N = 8$, $c_0 = -1$, and $L = 1$.

Figure 4. Analysis of exact and approximate solutions with error trends, for Eq (4.11).

Figure 4 gives both the exact and numerical solutions for Eq (4.11). The very small differences observed indicate the accuracy of the numerical approach. The error curves further confirm that the method is reliable and produces accurate results.

Figure 5 illustrates the absolute error as a function of the order M. The error decreases rapidly with increasing M, highlighting the spectral convergence of the Chelyshkov-based SHAM.

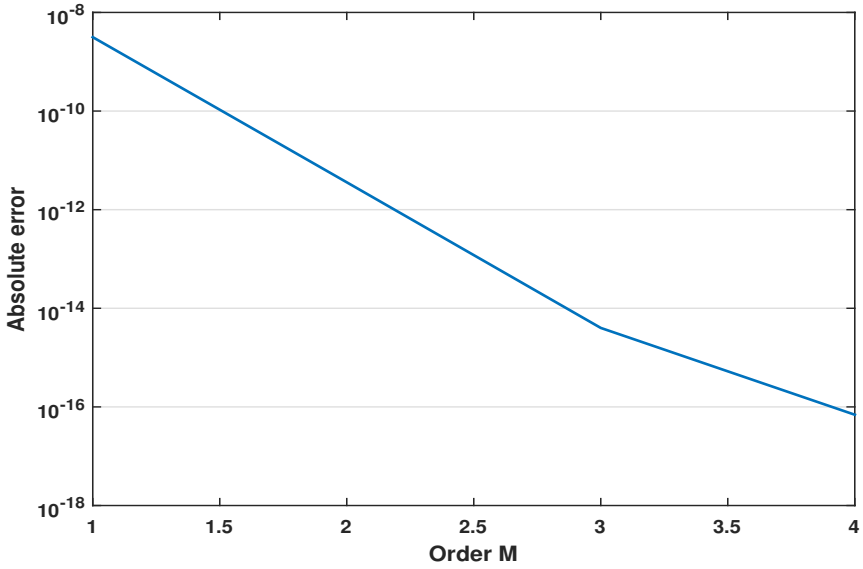

Figure 5. Absolute error vs. order M for $N = 8$, and $L = 1$ for Eq (4.11).

4.2. Linear case

Problem 3

We now consider a homogeneous Lane–Emden-type equation, as discussed in [4, 16, 18]:

$$y'' + \frac{2}{x}y' - 2(2x^2 + 3)y = 0, \quad x \in (0, L], \tag{4.15}$$

with $y(0) = 1$ and $y'(0) = 0$. The exact solution is $y(x) = \exp(x^2)$. Using the relation (4.5) gives

$$\frac{1}{L^2}u'' + \frac{2}{Lx}u' - 2(2x^2 + 3)u = \mathscr{H}(x) \tag{4.16}$$

such that

$$u(0) = u'(0) = 0,$$

where

$$\mathscr{H}(x) = -y_0'' - \frac{2}{x}y_0' - (4x^2 + 6)y_0 \quad \text{and} \quad y_0(x) = x^2 + 1.$$

The linear operator is defined as

$$\mathcal{L}(u) = \frac{1}{L^2}u'' + \frac{2}{Lx}u'.$$

By replacing $\mathcal{L}$ and $\mathscr{H}$ in Eq (3.17), we have

$$\mathcal{L}(u_k) = (\delta_k + c_0)\mathcal{L}(u_{k-1}) + c_0\left[-(1 - \delta_k)\mathscr{H} - 2(2x^2 + 3)u_{k-1}\right]. \tag{4.17}$$

Substituting Eqs (2.3) and (3.11) into Eq (4.17) gives

$$\mathbf{BA}_k = (\delta_k + c_0)\mathbf{BA}_{k-1} + c_0\left[-(1 - \delta_k)\mathbf{H} - 2(2x^2 + 3) \circ (\mathbf{C}(t)\mathbf{A}_{k-1})\right], \tag{4.18}$$

where

$$\mathbf{B} = \frac{1}{L^2}\mathbf{C}''(t) + diag(\frac{2}{Lx})\mathbf{C}'(x) - 2\mathbf{diag}(2x^2 + 3) \tag{4.19}$$

and

$$u_k(0) = u_k'(0) = 0.$$

Finally, we solve this system:

$$\begin{cases} \mathbf{A}_0 = \mathbf{B}^{-1}\bar{\mathbf{H}}, \\ \mathbf{A}_k = (\delta_k + c_0)\mathbf{B}^{-1}\bar{\mathbf{B}}\mathbf{A}_{k-1} + c_0\mathbf{B}^{-1}\left[-(1-\delta_k)\bar{\mathbf{H}} - 2(2x^2+3) \circ (\mathbf{C}(t)\mathbf{A}_{k-1})\right]. \end{cases} \tag{4.20}$$

Table 5. Error variation using the Chelyshkov-based SHAM, LT-HPM, and ADM, for $M = 4, L = 1$, and $N = 15$ for Eq (4.15).

x	Chelyshkov-based SHAM	LT-HPM [16], ADM [18]
0	0	0
0.01	4.4595×10^{-12}	0
0.04	2.6948×10^{-11}	0
0.10	3.2293×10^{-11}	1.2434×10^{-14}
0.17	3.5306×10^{-11}	3.0831×10^{-12}
0.25	3.7788×10^{-11}	1.9898×10^{-10}
0.35	4.6569×10^{-11}	5.3770×10^{-09}
0.45	7.3402×10^{-11}	7.8328×10^{-08}
0.55	5.6659×10^{-12}	7.1212×10^{-07}
0.65	7.3054×10^{-10}	4.4137×10^{-06}
0.75	1.4939×10^{-09}	1.9680×10^{-05}
0.83	5.1594×10^{-09}	6.5194×10^{-05}
0.90	3.3396×10^{-08}	1.6351×10^{-04}
0.96	8.4202×10^{-08}	3.1372×10^{-04}
0.99	1.3252×10^{-07}	4.6303×10^{-04}
1	1.5147×10^{-07}	5.2707×10^{-04}

Table 5 gives a comparative evaluation for absolute errors obtained by three different approaches: the proposed Chelyshkov-based SHAM approach, LT-HPM method, which is explained in [16], and ADM technique shown by [18]. The results show that the Chelyshkov-based SHAM yields the lowest error values, showing its clear advantage of decreasing computational error amounts. On top of that, the SHAM has a fast converging solution to precise answers, confirming its efficiency for problems requiring both high accuracy and fast computation.

Table 6 shows a direct comparison between numerical results obtained by the Chelyshkov-based SHAM, LT-HPM, and ADM with exact answers for problems at hand. From the results, one can see that the approximations from the proposed Chelyshkov-based SHAM have very high accuracy and are quite close to exact solution. It shows that the Chelyshkov-based SHAM gives higher precision and is more reliable than other techniques, which demonstrate its effectiveness in solving complex mathematical problems. Also, better accuracy in the Chelyshkov-based SHAM shows that it has strong potential for

further usage in situations that need very precise numerical estimation and fast convergence to optimal solutions.

Table 6. Comparison between the Chelyshkov-based SHAM, LT-HPM, ADM and the exact solution with $M = 4, L = 1$, and $N = 15$ for Eq (4.15).

x	Chelyshkov-based SHAM	LT-HPM [16], ADM [18]	Exact sol
0	1.000000000000000	1.000000000000000	1.000000000000000
0.0109	1.000119388969177	1.000119388964718	1.000119388964718
0.0432	1.001870343915754	1.001870343888806	1.001870343888806
0.0955	1.009160328478472	1.009160328446166	1.009160328446179
0.1654	1.027746600363419	1.027746600325030	1.027746600328113
0.2500	1.064494458955647	1.064494458718876	1.064494458917859
0.3455	1.126780418117939	1.126780412694419	1.126780418071369
0.4477	1.221973675452556	1.221973597050772	1.221973675379154
0.5523	1.356619280147169	1.356618568034100	1.356619280152835
0.6545	1.534771288801716	1.534766875817270	1.534771289532253
0.7500	1.755054655466403	1.755034977180114	1.755054656960298
0.8346	2.006715383484737	2.006650184084876	2.006715378325386
0.9045	2.266270743383852	2.266107204814253	2.266270709987778
0.9568	2.497809351479664	2.497495550209225	2.497809267278094
0.9891	2.659842824183984	2.659379657298854	2.659842691662801
1.0000	2.718281979931200	2.717754761889216	2.718281828459046

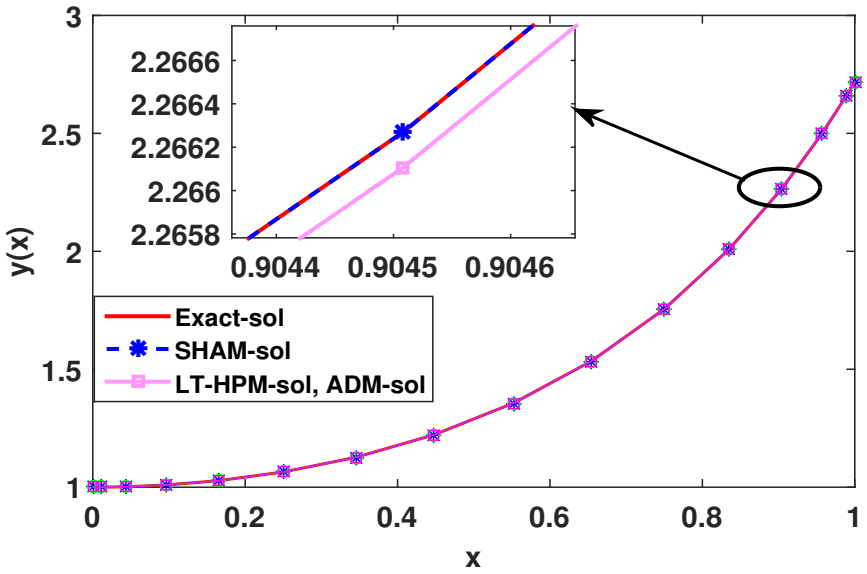

Figure 6. A review of the exact solution vs the approximations using the Chelyshkov-based SHAM, LT-HPM, and ADM for Eq (4.15).

Figure 6 shows the exact solution with approximation from three various approaches for comparing visually. All curves seem like they overlap in first view, but if we zoom in to any section of the graph,

we see that the Chelyshkov-based SHAM curve stays very near with the exact solution. The LT-HPM and ADM curves, on the other side, go away from that curve. That makes it more clear how the Chelyshkov-based SHAM has better precision and shows higher effectiveness for obtaining very precise numeric approximations, assuring its trust as means for solving hard mathematical questions.

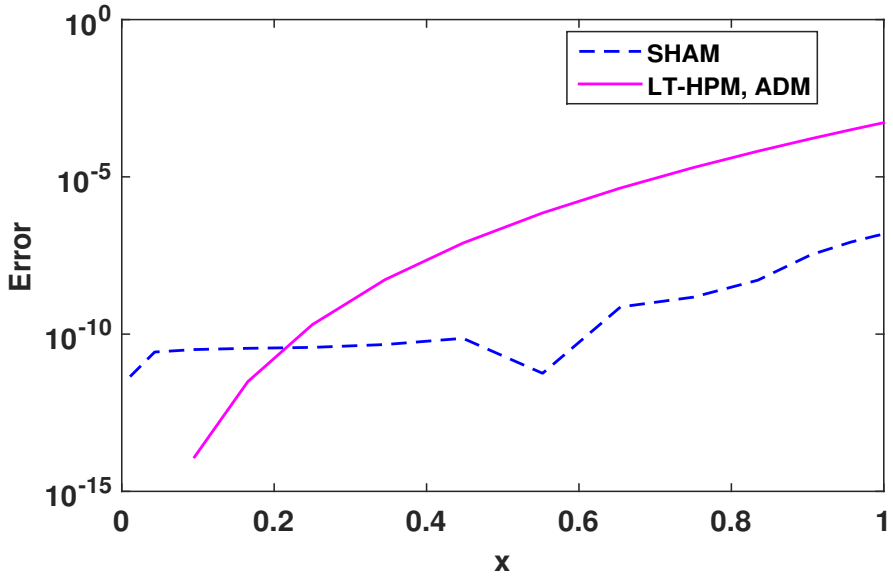

Figure 7. Comparison of errors using the Chelyshkov-based SHAM, LT-HPM, and ADM for Eq (4.15).

Figure 7 provides an extra proof of this outcome by presenting the related curves for errors. It is evidently visible that the Chelyshkov-based SHAM error stays much lower for every part of domain than the other two techniques. This means the Chelyshkov-based SHAM is highly precise and has a steady performance in reducing various computational errors, making it superior to usual numerical problem-solving ways.

Problem 4

Consider the following linear ordinary differential equation [4, 16, 18]:

$$y'' + \frac{8}{x}y' + xy = -30x + 44x^3 - x^4 + x^5, \quad x \in (0, L], \tag{4.21}$$

with $y(0) = 0$ and $y'(0) = 0$. The analytical solution is $y(x) = x^4 - x^3$. By applying the Chelyshkov-based SHAM and heeding the steps used in the previous examples, we ultimately get the following system:

$$\begin{cases} \mathbf{A}_0 = \mathbf{B}^{-1}\bar{\mathbf{H}}, \\ \mathbf{A}_k = (\delta_k + c_0)\mathbf{B}^{-1}\bar{\mathbf{B}}\mathbf{A}_{k-1} + c_0\mathbf{B}^{-1}\left[-(1-\delta_k)\bar{\mathbf{H}} + x \circ (\mathbf{C}(t)\mathbf{A}_{k-1})\right], \end{cases} \tag{4.22}$$

where

$$\mathbf{B} = \frac{1}{L^2}\mathbf{C}''(t) + \mathbf{diag}(\frac{8}{Lx})\mathbf{C}'(t) + \mathbf{diag}(x). \tag{4.23}$$

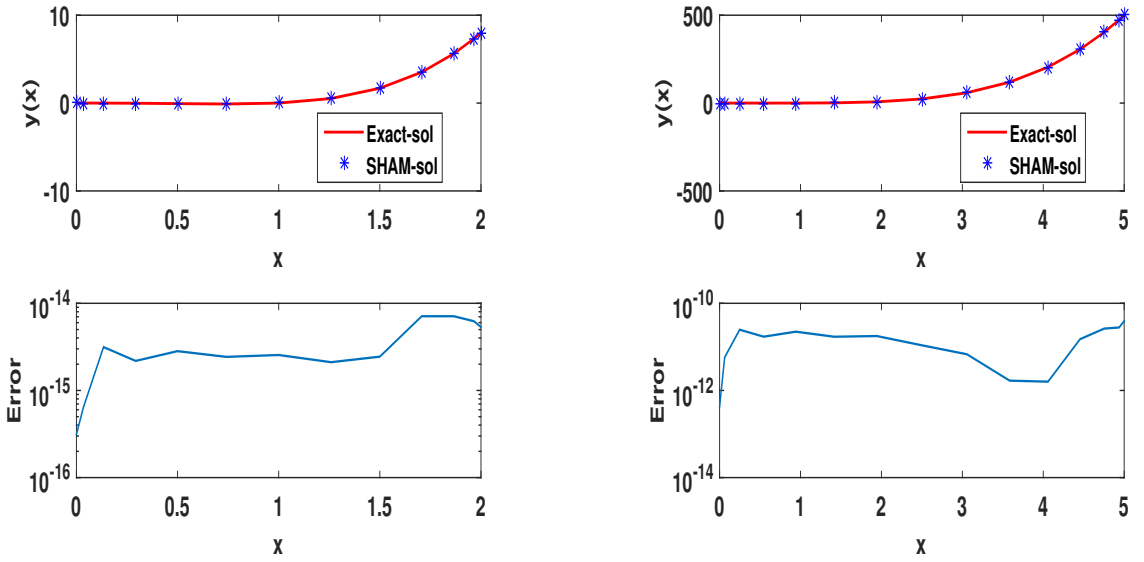

(a) $M = 8$, $N = 12$, $c_0 = -1$, and $L = 2$. **(b)** $M = 18$, $N = 14$, $c_0 = -0.86$, and $L = 5$.

Figure 8. Exact and approximate solutions with associated error behavior for Eq (4.21).

Figure 8 shows the exact and the Chelyshkov-based SHAM approximate solutions along with their corresponding absolute errors. In both cases, the approximate results closely match the exact solutions, while the errors remain very small over the entire domain.

Table 7. Evaluating the Chelyshkov-based SHAM against the exact solution for $L = 2$, and $N = 12$ for Eq (4.21).

x	$M = 2$ $c_0 = -1$	$M = 4$ $c_0 = -0.98$	$M = 6$ $c_0 = -0.98$	Exact sol
0,00	-0.00000000000000	-0.00000000000000	-0.00000000000000	0
0,03	-0.00003821495944	-0.00003821375774	-0.00003821376051	-0.00003821376050
0,13	-0.00208256768829	-0.00208256228698	-0.00208256229943	-0.00208256229943
0,29	-0.01776695677000	-0.01776695295773	-0.01776695296637	-0.01776695296637
0,50	-0.06250000488399	-0.06249999998924	-0.06250000000000	-0.06250000000000
0,74	-0.10538262249315	-0.10538261825424	-0.10538261826217	-0.10538261826216
1,00	-0.00000000412393	0.00000000000559	-0.00000000000001	-0.00000000000000
1,26	0.51628101093195	0.51628100311101	0.51628100312440	0.51628100312440
1,50	1.68750010127633	1.68749999996172	1.68750000000003	1.68750000000000
1,71	3.51776729034637	3.51776695305564	3.51776695296648	3.51776695296637
1,87	5.62708270380479	5.62708256266238	5.62708256229949	5.62708256229943
1,97	7.33913855727115	7.33913982927560	7.33913982889804	7.33913982889826
2,00	7.99999765554067	8.00000000026357	7.99999999999965	8.00000000000000

Table 7 displays calculated results from the Chelyshkov-based SHAM for different approximation degree orders and real ones. There is strong agreement, so the approach is considered reliable and

accurate. This agreement shows that the Chelyshkov-based SHAM has a strong ability to solve problems like these in a correct way.

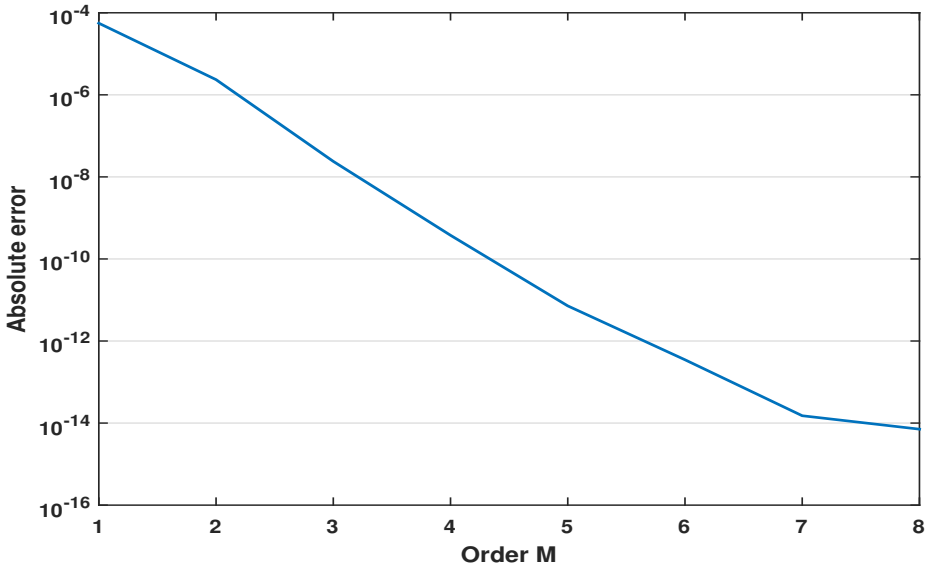

Figure 9. Absolute error vs order M for $N = 12$, and $L = 2$ for Eq (4.21).

Figure 9 illustrates the absolute error as a function of the order M. A rapid decay of the error is observed with increasing M, confirming the exponential convergence behavior of the proposed Chelyshkov-based SHAM.

Problem 5

Let us take the linear ordinary differential equation defined as follows [4, 16, 18]:

$$y'' + \frac{2}{x}y' + y = x^3 + x^2 + 12x + 6, \quad x \in (0, L], \tag{4.24}$$

with $y(0) = 0, y'(0) = 0$, and $y(x) = x^2 + x^3$. By employing the same approach and following the established methodology, the application of the Chelyshkov-based SHAM leads to the following results.

Figure 10 is made with three different parts and presents a comparison of both numerical and exact solutions over the interval $[0, 10]$. This is carried out using two different strategies: The Chelyshkov-based SHAM using Gauss–Lobatto points and the HFC technique. In the top left part, the Chelyshkov-based SHAM approximation is compared with the exact solution. Their matching suggests a good preciseness of the Chelyshkov-based SHAM. In the bottom left, the result estimated with the HFC is put together with the exact solution, and here a clear agreement is also observed, which shows the efficacy of this method. On the right side, the error curves of both techniques are displayed. It is evident that the Chelyshkov-based SHAM error is less than the HFC, indicating that the Chelyshkov-based SHAM is more accurate.

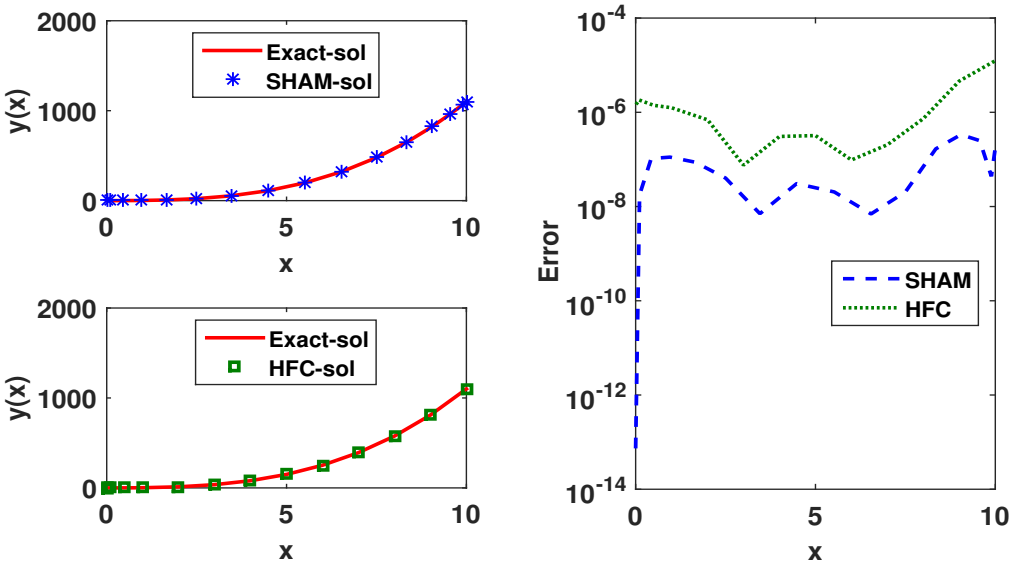

Figure 10. Visual representation of the exact solution alongside the Chelyshkov-based SHAM ($M = 20$, $N = 15$, $c_0 = -0.82$, and $L = 10$) and HFC approximations, including absolute error distributions for Eq (4.24).

Table 8. Error variation using the Chelyshkov-based SHAM and HFC method with $L = 10$ for Eq (4.24).

x	HFC error [4]	x	Chelyshkov-based SHAM error
0	0	0	7.36383×10^{-14}
0.01	1.47×10^{-06}	0.11	1.77180×10^{-08}
0.10	1.82×10^{-06}	0.43	1.04241×10^{-07}
0.50	1.41×10^{-06}	0.95	1.11839×10^{-07}
1.00	1.25×10^{-06}	1.65	8.73862×10^{-08}
2.00	6.93×10^{-07}	2.50	4.01795×10^{-08}
3.00	7.58×10^{-08}	3.45	7.06064×10^{-09}
4.00	3.07×10^{-07}	4.48	3.06738×10^{-08}
5.00	3.21×10^{-07}	5.52	2.03932×10^{-08}
6.00	9.74×10^{-08}	6.55	6.96787×10^{-09}
7.00	2.05×10^{-07}	7.50	2.03789×10^{-08}
8.00	7.36×10^{-07}	8.35	1.67647×10^{-07}
9.00	4.61×10^{-06}	9.05	3.35735×10^{-07}
10.00	1.24×10^{-05}	9.57	2.50299×10^{-07}
		9.89	4.37785×10^{-08}
		10.00	1.77181×10^{-07}

Table 8 gives a numerical check between errors from both the Chelyshkov-based SHAM and HFC schemes [4], which helps gain an exact assessment of how accurate these are. The Chelyshkov-based

SHAM that uses Gauss–Lobatto collocation points most often produces smaller errors if compared to an HFC, which actually uses Hermite collocation points over many chosen assessment points. The lowering of errors shows the better numerical performance of the Chelyshkov-based SHAM, which means it approximates the exact solution more closely. Also, the findings clearly indicate that the Chelyshkov-based SHAM is more stable and accurate than the HFC, so it is the efficient choice for this numerical type.

Remark. *The stable interval and optimal value of the convergence-control parameter c_0 for each considered problem are summarized in Table 9. These values make sure there is numerical stability with fast convergence for the Chelyshkov-based SHAM for selected order M, the count of collocation points N, and the scaling factor L.*

Table 9. Stable interval and optimal value of c_0 for different problems.

Problems	Stable interval of c_0	Optimal value of c_0	Order M	N	L	Absolute error $\mathcal{E}$
Problem 1	$-1.2 \le c_0 \le -0.2$	-1	4	15	1	2.65898×10^{-11}
Problem 2	$-1.25 \le c_0 \le -0.75$	-0.98	4	8	1	6.93889×10^{-17}
Problem 3	$-1.3 \le c_0 \le -0.9$	-1.02	4	15	1	1.5147×10^{-07}
Problem 4	$-1.25 \le c_0 \le -0.75$	-0.98	4	12	2	3.7734×10^{-10}
Problem 5	$-1.05 \le c_0 \le -0.5$	-0.82	20	15	10	3.3574×10^{-07}

5. Conclusions

This study adopted the Chelyshkov-based SHAM method to adress Lane–Emden-type equations, properly treating the singularity at $x = 0$ with confidence. Picking the right initial guess and an effective linear operator, paired with collocation points, makes the process smoother and significantly accelerates convergence. The parameter that controls convergence plays a crucial role, as it speeds up convergence, ensures stability and accuracy. Using numerical experiments, we evaluated the error behavior of the proposed approach, making a comparison against the ADM, LT-HPM, as well as HFC. The findings consistently show that our approach gives better results compared to these traditional methods and obtains more accuracy while using less computational costs. Of special note, the method uses fewer collocation points while maintaining exponential convergence, which is higher than wavelet-based strategies. Outside current results, the framework has built-in flexibility, so it can be expanded for Lane–Emden equations systems also in fractional-order models without difficulty. This flexibility opens promising avenues for further research for more difficult astrophysics models in the future.

Use of AI tools declaration

The authors declare they have not used Artificial Intelligence (AI) tools in the creation of this article.

Acknowledgments

Authors are thankful to Prince Sultan University for APC and support through TAS research lab.

Conflict of interest

The authors declare there is no conflict of interest.

Author contributions

M. Bouakkaz, N. Arar, M. Meflah, K. Shah, B. Abdalla and T. Abdeljawad: Writing – review and editing, Writing – original draft, Software, Conceptualization, Formal analysis, Methodology.

References

1. R. Kippenhahn, A. Weigert, A. Weiss, *Stellar Structure and Evolution*, Springer Berlin, Heidelberg, 2012. https://doi.org/10.1007/978-3-642-30304-3
2. H. J. Lane, On the theoretical temperature of the sun, under the hypothesis of a gaseous mass maintaining its volume by its internal heat, and depending on the laws of gases as known to terrestrial experiment, *American J. Sci.*, **2** (1870), 57–74. https://doi.org/10.2475/ajs.s2-50.148.57
3. O. W. Richardson, *The Emission of Electricity from Hot Bodies*, Longmans, Green and Company, 1921. Available from: https://archive.org/download/emissionelectricity00richrich.
4. K. Parand, M. Dehghan, A. R. Rezaei, S. M. Ghaderi, An approximation algorithm for the solution of the nonlinear Lane–Emden type equations arising in astrophysics using Hermite functions collocation method, *Comput. Phys. Commun.*, **181** (2010), 1096–1108. https://doi.org/10.1016/j.cpc.2010.02.018
5. W. M. Abd-Elhameed, H. M. Ahmed, M. A. Zaky, R. M. Hafez, A new shifted generalized Chebyshev approach for multi-dimensional sinh-gordon equation, *Phys. Scr.*, **99** (2024), 095269. https://doi.org/10.1088/1402-4896/ad6fe3
6. H. Khan, J. Alzabut, D. Baleanu, G. Alobaidi, M. U. Rehman, Existence of solutions and a numerical scheme for a generalized hybrid class of n-coupled modified ABC-fractional differential equations with an application, *AIMS Math.*, **8** (2023), 6609–6625. https://doi.org/10.3934/math.2023334
7. H. Ahmed, Solutions of 2nd-order linear differential equations subject to Dirichlet boundary conditions in a Bernstein polynomial basis, *J. Egypt. Math. Soc.*, **22** (2014), 227–237. https://doi.org/10.1016/j.joems.2013.07.007
8. M. Usman, H. U. Khan, M. Sarwar, N. Fatima, K. Abodayeh, An innovative analytical result of two-dimensional heat equation using joint mechanism of natural transform and Adomian decomposition method, *Eur. J. Pure Appl. Math.*, **18** (2025), 6051. https://doi.org/10.29020/nybg.ejpam.v18i2.6051
9. S. Singha, V. K. Sharmaa, Extended Bernoulli wavelet approximation method and its applications in solving the Lane–Emden differential equation and linear integral equation, *Filomat*, **38** (2024), 10071–10084. https://doi.org/10.2298/FIL2428071S
10. Y. Youssri, W. Abd-Elhameed, E. Doha, Ultraspherical wavelets method for solving Lane–Emden type equations, *Rom. J. Phys.*, **60** (2015), 1298–1314. Available from: https://rjp.nipne.ro/2015_60_9-10/RomJPhys.60.p1298.pdf.

11. W. M. A. Elhameed, Y. H. Youssri, E. H. Doha, New solutions for singular Lane–Emden equations arising in astrophysics based on shifted ultraspherical operational matrices of derivatives, *Comput. Methods Differ. Equ.*, **2** (2014), 171–185. Available from: https://www.researchgate.net/publication/277912947.
12. M. Al-Mazmumy, A. Alsulami, H. Bakodah, N. Alzaid, Modified Adomian method for the generalized inhomogeneous Lane–Emden-type equations, *Nonlinear Anal. Differ. Equ.*, **10** (2022), 15–35. https://doi.org/10.12988/nade.2022.91142
13. M. Abdelhakem, Y. Youssri, Two spectral Legendre's derivative algorithms for Lane–Emden, Bratu equations, and singular perturbed problems, *Appl. Numer. Math.*, **169** (2021), 243–255. https://doi.org/10.1016/j.apnum.2021.07.006
14. S. G. Hosseini, S. Abbasbandy, Solution of Lane–Emden type equations by combination of the spectral method and Adomian decomposition method, *Math. Probl. Eng.*, **2015** (2015), 1–10. https://doi.org/10.1155/2015/534754
15. M. Chapwanya, R. Dozva, G. Muchatibaya, A nonstandard finite difference technique for singular Lane–Emden type equations, *Eng. Comput.*, **36** (2019), 1566–1578. https://doi.org/10.1108/EC-08-2018-0344
16. R. Tripathi, H. Mishra, Homotopy perturbation method with Laplace transform (LT-HPM) for solving Lane–Emden type differential equations (LETDEs), *SpringerPlus*, **5** (2016), 1859. https://doi.org/10.1186/s40064-016-3487-4
17. A. M. Wazwaz, A new algorithm for solving differential equations of Lane–Emden type, *Appl. Math. Comput.*, **118** (2001), 287–310. https://doi.org/10.1016/S0096-3003(99)00223-4
18. A. M. Wazwaz, A new method for solving singular initial value problems in the second-order ordinary differential equations, *Appl. Math. Comput.*, **128** (2002), 45–57. https://doi.org/10.1016/S0096-3003(01)00021-2
19. A. M. Wazwaz, The variational iteration method for solving nonlinear singular boundary value problems arising in various physical models, *Commun. Nonl. Sci. Num. Simul.*, **16** (2011), 3881–3886. https://doi.org/10.1016/j.cnsns.2011.02.026
20. S. Liao, A new analytic algorithm of Lane–Emden type equations, *Appl. Math. Comput.*, **142** (2003), 1–16. https://doi.org/10.1016/S0096-3003(02)00943-8
21. O. Arqub, A. El-Ajou, A. S. Bataineh, I. Hashim, A representation of the exact solution of generalized Lane–Emden equations using a new analytical method, *Abstr. Appl. Anal.*, **2013** (2013), 378593. https://doi.org/10.1155/2013/378593
22. S. Iqbal, A. Javed, Application of optimal homotopy asymptotic method for the analytic solution of singular Lane–Emden type equation, *Appl. Math. Comput.*, **217** (2011), 7753–7761. https://doi.org/10.1016/j.amc.2011.02.083
23. C. Li, Q. Luo, G. Meng, X. Liu, A fast Chebyshev collocation method for stability analysis of a robotic machining system with time delay, *J. Comput. Nonlinear Dyn.*, **20** (2024), 011006. https://doi.org/10.1115/1.4067062

24. E. Doha, W. Abd- Elhameed, Y. Youssri, Second kind Chebyshev operational matrix algorithm for solving differential equations of Lane–Emden type, *New Astron.*, **23–24** (2013), 113–117. https://doi.org/10.1016/j.newast.2013.03.002

25. H. M. Ahmed, Enhanced shifted Jacobi operational matrices of derivatives: Spectral algorithm for solving multiterm variable-order fractional differential equations, *Bound Value Probl.*, **2023** (2023), 108. https://doi.org/10.1186/s13661-023-01796-1

26. M. Izadi, P. Roul, An effective numerical algorithm for coupled systems of Emden–Fowler equations via shifted airfoil functions of the first kind, *Math. Model. Anal.*, **29** (2024), 781–800. https://doi.org/10.3846/mma.2024.19540

27. Y. H. Youssri, A. G. Atta, Spectral collocation approach via normalized shifted Jacobi polynomials for the nonlinear Lane–Emden equation with fractal-fractional derivative, *Fractal Fract.*, **7** (2023), 133. https://doi.org/10.3390/fractalfract7020133

28. A. Benzahi, N. Arar, N. Abada, M. Rhaima, L. Mchiri, A. Ben Makhlouf, Numerical investigation of Fredholm fractional integro-differential equations by least squares method and compact combination of shifted Chebyshev polynomials, *J. Nonlinear Math. Phys.*, **30** (2023), 1392–1408. https://doi.org/10.1007/s44198-023-00128-2

29. Z. Laouar, N. Arar, A. Ben Makhlouf, Theoretical and numerical study for Volterra–Fredholm fractional integro-differential equations based on Chebyshev polynomials of the third kind, *Complexity*, **2023** (2023), 6401067. https://doi.org/10.1155/2023/6401067

30. N. Arar, B. Deghdough, S. Dekkiche, Z. Torch, A. M. Nagy, Numerical solution of the Burgers' equation using Chelyshkov polynomials, *Int. J. Appl. Comput. Math.*, **10** (2024), 33. https://doi.org/10.1007/s40819-023-01663-8

31. Z. Laouar, N. Arar, A. Talaat, Efficient spectral Legendre Galerkin approach for the advection diffusion equation with constant and variable coefficients under mixed Robin boundary conditions, *Adv. Theory Nonlinear Anal. Appl.*, **7** (2023), 133–147. https://doi.org/10.31197/atnaa.1139533

32. M. Izadi, P. Roul, A new approach based on shifted Vieta–Fibonacci-quasilinearization technique and its convergence analysis for nonlinear third-order Emden–Fowler equation with multi-singularity, *Commun. Nonlinear Sci. Numer. Simul.*, **117** (2023), 106912. https://doi.org/10.1016/j.cnsns.2022.106912

33. F. A. Shah, Kamran, W. Boulila, A. Koubaa, N. Mlaiki, Numerical solution of advection-diffusion equation of fractional order using Chebyshev collocation method, *Fractal Fract.*, **7** (2023), 762. https://doi.org/10.3390/fractalfract7100762

34. S. S. Motsa, P. Sibanda, S. Shateyi, A new spectral-homotopy analysis method for solving a nonlinear second order BVP, *Commun. Nonlinear Sci. Numer. Simul.*, **15** (2010), 2293–2302. https://doi.org/10.1016/j.cnsns.2009.09.019

35. S. J. Liao, *Beyond Perturbation: Introduction to the Homotopy Analysis Method*, Chapman and Hall/CRC, New York, 2003, https://doi.org/10.1201/9780203491164

36. S. Liao, *Homotopy Analysis Method in Nonlinear Differential Equations*, Springer, Berlin, Heidelberg, 2012, https://doi.org/10.1007/978-3-642-25132-0

37. W. Fafa, Z. Odibat, N. Shawagfeh, The homotopy analysis method for solving differential equations with generalized Caputo-type fractional derivatives, *J. Comput. Nonlinear Dyn.*, **18** (2022), 021004. https://doi.org/10.1115/1.4056392

38. Z. Odibat, S. Kumar, A robust computational algorithm of homotopy asymptotic method for solving systems of fractional differential equations, *J. Comput. Nonlinear Dyn.*, **14** (2019), 081004. https://doi.org/10.1115/1.4043617

39. V. S. Chelyshkov, Alternative orthogonal polynomials and quadratures, *Electron. Trans. Numer. Anal.*, **25** (2006), 17–26. Available from: https://etna.ricam.oeaw.ac.at/volumes/2001-2010/vol25.

40. E. Gokmen, G. Yuksel, M. Sezer, A numerical approach for solving Volterra type functional integral equations with variable bounds and mixed delays, *J. Comput. Appl. Math.*, **311** (2017), 354–363. https://doi.org/10.1016/j.cam.2016.08.004

41. M. Bouakkaz, N. Arar, M. Meflah, Enhanced numerical resolution of the Duffing and Van der Pol equations via the spectral homotopy analysis method employing Chebyshev polynomials of the first kind, *J. Appl. Math. Comput.*, **71** (2025), 1159–1187. https://doi.org/10.1007/s12190-024-02271-5

42. S. J. Liao, *Advances in the Homotopy Analysis Method*, Word Scientific, Singapore, 2014. https://doi.org/10.1142/8939

43. S. S. Motsa, Z. G. Makukula, The spectral-homotopy analysis method (SHAM) for solutions of boundary layer problems, in *Applications of Heat, Mass and Fluid Boundary Layers* (eds. R. Fagbenle, O. Amoo, S. Aliu, A. Falana), Woodhead Publishing, (2020), 133–148. https://doi.org/10.1016/B978-0-12-817949-9.00014-1

44. P. Sibanda, S. S. Motsa, Z. G. Makukula, A spectral-homotopy analysis method for heat transfer flow of a third grade fluid between parallel plates, *Int. J. Numer. Methods Heat*, **22** (2012), 4–23. https://doi.org/10.1108/09615531211188766

AIMS Press